Proceedings of the Institute of Acoustics

SHORT RANGE MULTIPATH REJECTION IN A BOUNDED CHANNEL USING A VERTICAL LINE ARRAY

P. Walmsley and S.A.S. Jones

THORN EMI Electronics Limited, Naval Systems Division, Albert Drive, Sheerwater, Woking, Surrey, GU21 5RU.

INTRODUCTION

The majority of shallow water propagation studies are concerned with the pressure field at a large distance from the source compared with the water depth ie. $r > 10h$ (Ref. 1). This paper however considers shorter range propagation (for which $r < 5h$) and the use of simple directionality in a vertical receiving array to reduce signal fluctuation by rejecting surface and bottom reflected energy. Effective isolation of the direct ray path means that a simple spherical spreading law can be applied and hence the vertical array can be used for CW transducer calibration at 'long' range, rejection of surface generated sea noise and the noise measurement of vessels underway without knowledge of bottom parameters.

In this paper, an ideal homogenous channel is examined with a hard, perfectly reflecting bottom and smooth free surface. Ray and mode summation down the channel from a single point source are used to compute the response of a vertical array with discrete point receiving elements. Linear element summation (beamforming), shading and intensity summation methods are explored as a function of source-receiver range and the results compared with a scale model in an acoustic tank. The output of the array shows good agreement with the predicted results from which the range of spherical spreading can be defined. Finally, the implementation of a versatile vertical array configuration for practical measurements is described.

RAY MODE MODELLING

In a layer with a pressure release surface and a hard perfectly-reflecting bottom, the equivalence between ray theory with a network of image sources and the normal mode representation with pairs of upward and downward propagating plane waves is well known. At short ranges the normal mode representation must include a set of discrete modes and a continuous contribution due to rays striking the bottom at angles closer to the normal than the critical grazing angle. For long range propagation only discrete modes are important and for a perfectly reflecting lower boundary there is no continuous component.

THE SIMPLE RAY MODEL

Referring to Brekhovskikh and Lysanov (Ref. 2, Ch. 5), the multiple reflections in an ideal shallow water channel may be replaced by an infinite sum of image sources. The pressure at any horizontal range r and depth z is then given by the sum of all images which for convenience are grouped into sets of 4 rays:

$$P(r,z) = \sum_{l=0}^{\infty} [(-V_{l1})^{l}(\exp(jkR_{l1})/R_{l1}) + (-V_{l2})^{(l+1)}(\exp(jkR_{l2})/R_{l2}) - (-V_{l3})^{l}(\exp(jkR_{l3})/R_{l3}) - (V_{l4})^{(l+1)}(\exp(jkR_{l4}/R_{l4})] \qquad (1)$$

Here l is the index of summation, k is the wave number ($=2\pi/\lambda$), V_{lq} is the complex bottom reflection coefficient for ray (l,q) and R_{lq} is the path length of each ray (l,q). The ray path lengths are given by:

$$R_{lq} = \sqrt{r^2 + z^2_{lq}} \qquad q = 1 \text{ to } 4 \tag{2}$$

where

$$\begin{aligned} z_{l1} &= 2hl + z_1 - z \\ z_{l2} &= 2h\,(l + 1) - z_1 - z \\ z_{l3} &= 2hl + z_1 \\ z_{l4} &= 2h\,(l + 1) - z + z \end{aligned} \tag{3}$$

in which h is the channel depth and z_1 is the source depth. If it is assumed that the channel is overlying a fluid bottom, the reflection coefficient V_{lq} is given by:

$$V_{lq} = \frac{m \cos \theta_{lq} - \sqrt{n^2 - \sin^2\theta_{lq}}}{m \cos \theta_{lq} + \sqrt{n^2 - \sin^2\theta_{lq}}} \tag{4}$$

where $m = \rho_1/\rho$ is the ratio of bottom density to water density and $n = c/c_1$, is the ratio of sound speed in the water to sound speed in the bottom, assumed real. The angle of incidence θ_{lq} between each ray and the bottom normal is:

$$\theta_{lq} = \tan^{-1}\,(z_{lq}/r) \tag{5}$$

For angles of incidence such than $n < \sin\theta_{lq}$, then the modulus of the reflection coefficient $|V_{lq}| = 1$ and the phase is given by:

$$\emptyset_{lq} = -2 \tan^{-1}\left(\frac{\sqrt{\sin^2\theta_{lq} - n^2}}{m \cos \theta_{lq}}\right) \tag{6}$$

The surface reflection coefficient is taken as $-1\angle 0^\circ$, and under these conditions the channel is lossless. Equations (1) - (6) are then easily solved by computer to give the pressure amplitude and phase from any defined source at any point in the channel.

THE MODE MODEL

The channel studied in this paper has a hard bottom with density $\rho_1 = 7700$ kgm^{-3} and a compressional sound speed c_1 of 6100 ms^{-1}. The transmission into this steel plate is small even at incident ray angles less than the critical grazing angle. It is therefore assumed that the bottom is perfectly reflecting, which means that the field is exactly represented by the discrete modal spectrum.

The solution of the wave equation giving the acoustic pressure for a harmonic source is usually written as:

$$P = \rho \exp [j(\omega t+\pi/4)]\, r^{-\frac{1}{2}} \sum_m q_m \sin\gamma_m z_o \sin \gamma_m z \exp(-jk_m r) \qquad (7)$$

where the source excitation function $q_m = \dfrac{2\pi(\rho c \Pi)^{\frac{1}{2}}}{[\nu_m \sqrt{k_m}]}$

and $\nu_m = \int_o^h \rho_o \sin^2(\gamma_m z)dz$

where Π is the source power

$\gamma_m = (m-\frac{1}{2})/h$

$k = \sqrt{k_m^2 - \nu_m^2} = \omega^2/c^2$

m is the mode number

This representation applies to distances that are large compared with the wavelength (ie. $|k_m r|>>1$), since it contains the asymptotic approximation for the Hankel function. It can be seen from Equation (7) that the phase of the received signal is invariant with depth and the response of the vertical line array is determined by summing over z for each mode.

THE VERTICAL LINE ARRAY

A vertical line array in a bounded channel can be used in a number of ways to reduce signal pressure fluctuations due to multipath interference. For an array of N elements, the methods described in terms of the normalized power output, A are:

Intensity $$A = 1/N \sum_{i=1}^{N} (M_o P_i)^2 \qquad (8)$$

Beamforming $$A = (1/N \sum_{i=1}^{N} M_o P_i)^2 \qquad (9)$$

where M_o is the (constant) sensitivity of each array element and P_i is the acoustic pressure at the i'th element. Additionally, the beamforming technique can be extended to include amplitude shading and focussing. Mode matching could also be used, but is difficult to implement in practice.

Intensity

Following Urick (Ref. 3), the average intensity law in the ideal lossless channel may be obtained by replacing the infinite sum of image sources with a continuous line of image sources having the source density equal to I_o/h per unit length of line.

The total intensity at range r is given by:

$$I_r = \frac{I_o}{h} \int_{-\infty}^{\infty} \frac{dh'}{r^2 + h'^2} = \frac{\pi I_o}{rh} \qquad (10)$$

The average cylindrical spreading law is then just:

$$P^2_{CYL} = \pi/rh \qquad (11)$$

which, it should be noted, differs from the net outward intensity by spreading spherical power over a cylindrical surface.

$$P^2_{HORIZ} = 2/rh \qquad (12)$$

Beamforming

In the general focussed case of a uniformly weighted array the closest approach of a source which exhibits spherical spreading, is limited to the 'far field' array distance. For an array focussed at r_o, this near limit r_1 is given by:

$$r_1 = 1/(1/r_o + 1/r') \qquad (13)$$

where r' is the far field limit of an unfocussed array of length d

$$r' = d^2/\lambda \qquad (14)$$

and corresponds to a maximum path difference to all elements of the array of $\lambda/8$. The farthest distance r_2 from the array is limited either by surface and bottom reflected rays appearing inside the main lobe or by the depth of field of the focussed array. In practice, the limitation is likely to be the former condition for which the geometry is easily computed. The distance r_2 however is a maximum when the array is at mid water when

$$r_2 = h\sqrt{d^2/\lambda - 1} \qquad (15)$$

where h is the channel depth. Furthermore for the source to remain within the -3 dB points of the array beam, its vertical position about the array centre must vary by no more than

$$z = \pm r \tan(\lambda/d) \simeq r\lambda/d \text{ for small } \lambda/d \qquad (16)$$

Hence, to estimate the source level of a point transmitter in a bounded medium using a beamformed array and assuming spherical spreading, the source must satisfy four conditions:

1. The far field array limit, r_1 (Equation 13)
2. The beamwidth limit, r_2 (Equation 15)
3. The allowable error in source depth (Equation 16)
4. The available signal-to-noise ratio as determined by the source level and array gain.

EXPERIMENT

In order to illustrate direct ray path measurement in a bounded medium, an experiment was devised in which the range of an omni-directional source from a vertical array could be varied in a model tank.

The layout of the experiment is shown in Figure 1 in which a steel sheet measuring 1.82 x 0.5 x 0.01 m was suspended at a depth of 0.28 m below the water surface to simulate a hard, perfectly reflecting bottom. Two large foam baffles were set at 45° to the water surface on either side of the steel plate to reduce tank wall reflections. 50 kHz and 100 kHz were chosen as suitable (practical) frequencies at which to operate and if the channel represents a depth of 100 m, the corresponding scale frequencies are approximately 150 Hz and 300 Hz.

A spherical projector with a radial resonance of 60 kHz and omni-directional response to within ± 2 dB at 100 kHz was mounted on an adjustable shaft and horizontal guide rod to give free motion along the length of the bed plate at a mid-water depth of 0.14 m. A ceramic array of nominal length 110 mm and consisting of 10 elements each measuring approximately 10 mm long by 5 mm x 5 mm and spaced 1.5 mm apart was mounted with its centre at mid water below the horizontal guide rod at one end of the steel plate. The beamwidths of this array were 13° at 50 kHz and 7° at 100 kHz and were well behaved with -13 dB sidelobes indicating uniform phase response.

To avoid inducing mechanical noise in the array, the projector was arranged to move relative to the receiver. A cord attached between the projector guide mechanism, a winding handle and a pulley and weight allowed accurate control of the projector distance over a range of 0.2 m to 1.4 m corresponding to scale ranges of about 66 m and 466 m. A 10 turn potentiometer was attached to the pulley wheel and connected to the x-axis input of the B&K chart recorder to give a pen displacement directly proportional to projector range. The array output was fed via a B&K measuring amplifier to the logarithmic y-axis input of the chart recorder and hence the action of turning the handle produced a direct plot of array response in decibels against projector range.

To reduce tank reverberation, a 'pseudo continuous' wave technique was adopted in which a transmit pulse of 4 ms was used with a narrow receive gate of 50-100 µs delayed by 3.9 ms from the start of the transmit pulse. In this way, all ray paths with a travel time of up to 4 ms will be sampled which allows up to 21 reflected ray pairs to be included down the channel, the last ray pair adding only 1.3 dB to a source at 1 m range. In this way, the output of the array and that of a single, central, omni-directional element were each recorded at frequencies of 50 kHz and 100 kHz for a source range of 0.2 to 1.3 m. The results are shown in Figures 2 to 5.

COMPUTER MODEL

In order to verify the performance of the model tank experiment, computer simulations using the ray and mode methods were devised. The programs compute the pressure amplitude and phase at any range and depth for a source point of given depth and frequency using Equations (1 to 6) or Equation (7). Although strictly only applicable to fluid boundaries, Equations (4 to 6) were used at the bottom interface with the density and compressional wave speed as for steel due to the difficulty of shear wave treatment.

At each range point, the pressure field is summed over all array elements on a coherent, weighted coherent or incoherent basis to give beamformed or intensity outputs. Following trial runs of the programs, it was discovered that the structure of the response could be adequately modelled with range points at $\lambda/3$ spacing. The results of the ray method including a spherical spreading law curve, for 50 kHz and 100 kHz and single hydrophone and beamformed array outputs are shown in Figures 6 to 9 in direct comparison with Figures 2 to 5. Figure 10 shows the effect of binomial shading of the array at 50 kHz whilst Figure 11 shows the predicted intensity response compared with cylindrical spreading. In each case, the source, reference hydrophone and array centre are all at mid-water depth. Similar results for the mode method are in close agreement.

RESULTS AND DISCUSSION

From the results in Figures 2 to 6, it is apparent that the measured array response shows a much higher order of spatial fluctuations than the computed response. This effect was mainly observed using the 'pseudo-continuous' experimental method and may possibly arise from multiple reflection within the steel bed plate. The precise cause however has not been identified.

The measured array response at 50 kHz in Figure 2 begins to deviate from the spherical spreading law below a range of 0.3 m and above 1.1 m range. The lower range results from the far field array limitation calculated at 0.43 m from Equation (14) whilst the upper bound shows the effect of interference between direct and reflected rays beyond a calculated range of 1.02 m (from Equation (16). Over the range 0.4 m to 1.0 m it can be seen that the total response lies within ± 4 dB of a spherical spreading law compared with the single hydrophone responses in Figures 3 and 7 which exhibit a spread of ± 12 dB. The use of the vertical array has therefore improved the accuracy of measurement by ± 8 dB and spherical law curve fitting could reduce variation still further to ± 2 dB or better.

Similar results for mid-channel projector and receiver positions at 100 kHz are shown in Figures 4, 8, 5 and 9. With the exception of two nulls at around 0.7 m, the measured array response in Figure 4 again is within ± 4 dB of the spherical spreading law. Deviation is seen to occur below about 0.5 m whilst the calculated far field distance r_1, is 0.86 m and the beamwidth limit r_2 is 2.1 m. In each case, good agreement in depth of interference is obtained between computed and measured results.

Although not shown, computed and measured results have also been obtained for the source at 1/4 and 3/4 of the channel depth (with the array centred at mid-channel). The array response is now poorer than the source at mid-channel though still showing 15-20 dB less variation than the single reference hydrophone. As expected, best results are obtained with the source well within the main beam of the array with little side-lobe contribution. Figure 10 illustrates this point for the computed output of a binomial weighted array at

50 kHz (with the source at mid-water) in which the side-lobes have been eliminated. Excellent agreement to ±1 dB about spherical spreading is obtained from below 0.2 m up to 1.05 m despite the wider beamwidth compared with a linear weighting.

Finally, Figure 11 shows the computed result at 50 kHz and mid-water of summing all 10 hydrophones incoherently according to the intensity method of Equation (8). The cylindrical spreading law of Equation (12) is superimposed. This result should be compared with Figure 6 showing more rapid fluctuations and slightly greater deviation about the spreading law. Although there are now no near or far field limitations and further results have shown that the intensity method is far more tolerant of source and receiver depth, it should be remembered that an average spreading curve can only be applied to intensity measurements when bottom losses are known.

A PRACTICAL VERTICAL ARRAY

A practical vertical hydrophone array covering a broad frequency band is naturally subject to changes in beamwidth, minimum operating range and maximum operating range. Constant beamwidth schemes such as log periodic element spacing may be employed at the expense of an increase in electronic processing complexity or versatility may be retained with a larger number of ceramic elements spaced half a wavelength apart at the highest operating frequency. Unfortunately, this latter option is complex and time consuming to construct. With the advent of PVDF however, a third possibility of extended elements now exists in which the number of elements is determined largely by the ability to switch between active sections and the highest frequency defines the minimum element spacing.

Such an experimental array, of length 2.5 m, diameter 25 mm and comprising 10 elements, each of active length 180 mm has been constructed. This geometry gives a beamwidth of 30^{o} at 1 kHz and a maximum range r_2 at 1 kHz, of 178 m. The full array might therefore be expected to be useful over the range of 1-10 kHz. Below 1 kHz, the maximum range r_2 is too close and above about 10 kHz the beamwidth is too small for stability unless elements are switched out.

Each element of the array uses a novel construction developed by Raychem (Ref. 4) in which a helical wire of PVDF is wrapped around a compliant former which is itself filled with a low bulk modulus elastomer. This design lends itself to a coaxial construction and the miniature cable for each element together with strain relief Kevlar tape is brought out through the centre of all subsequent elements. Each element is then overmoulded in polyurethane and the entire array protected in a heat shrink jacket. All the wires at one end of the array are taken through a water-blocked connector into an aluminium preamplifier vessel. A four core power supply and signal cable complete the assembly at the preamplifier end whilst an anchor ring is provided at the other end for attachment of a buoy or weight.

In this form, the element sensitivity is -186 ± 2 dB re 1 V/μPa over the frequency range dc to 7 kHz with element-to-element variation of less than 1 dB. The array has also been tested to a pressure equivalent to 200 m of water with less than 1 dB change in sensitivity. The narrow profile and a preamplifier pole at 500 Hz should help to reduce susceptibility to wave motion though trials at sea have yet to be carried out.

CONCLUSIONS

Reduction of multipath interference in a shallow water tank experiment has been set up at 1/333 scale corresponding to a real channel of depth 100 m and operating frequencies of 150 Hz and 300 Hz. Using the beamforming technique, the range of operation is limited by the nearfield of the array and multiple reflections within the main beam, however, between these limits all measurements fall with ±4 dB of the spherical spreading law compared with ±12 dB for a single hydrophone. Predictions from ray and mode computer models show that the intensity method produces similar variation about a cylindrical spreading law and is more tolerant of source depth though for practical use the bottom loss must be known.

With a knowledge of the limitations it is suggested that a vertical beamforming array is a useful tool for shallow water, short range signal measurements. The implementation of such an array has been described using 10 x 180 mm long helical PVDF elements over 2.5 m to achieve a bandwidth of 7 kHz at a sensitivity of -186 dB re 1 V/μPa. Tests at sea are now necessary to verify performance.

ACKNOWLEDGEMENTS

In carrying out the work described in this paper, recognition should be given to the following organizations for their assistance and support: University of Bradford, DBE Technology Limited, SERC, ARE (Teddington), THORN EMI Electronics Limited and Raychem Limited.

REFERENCES

[1] R.J. Urick, Sound Propagation in the Sea, Peninsula Publishing, 1982.

[2] L.M. Brekhovskikh, Yu. Lysanov, Fundamentals of Ocean Acoustics, Springer Verlag, London 198.

[3] R.J. Urick, J.A.S.A., 46(3) (Part 2), 1969, pp 780-788.

[4] D. Fox et al, An extended acoustic sensor using a new piezoelectric cable, IEEE Ultrasonics Symposium, Williamsburg, November 1986.

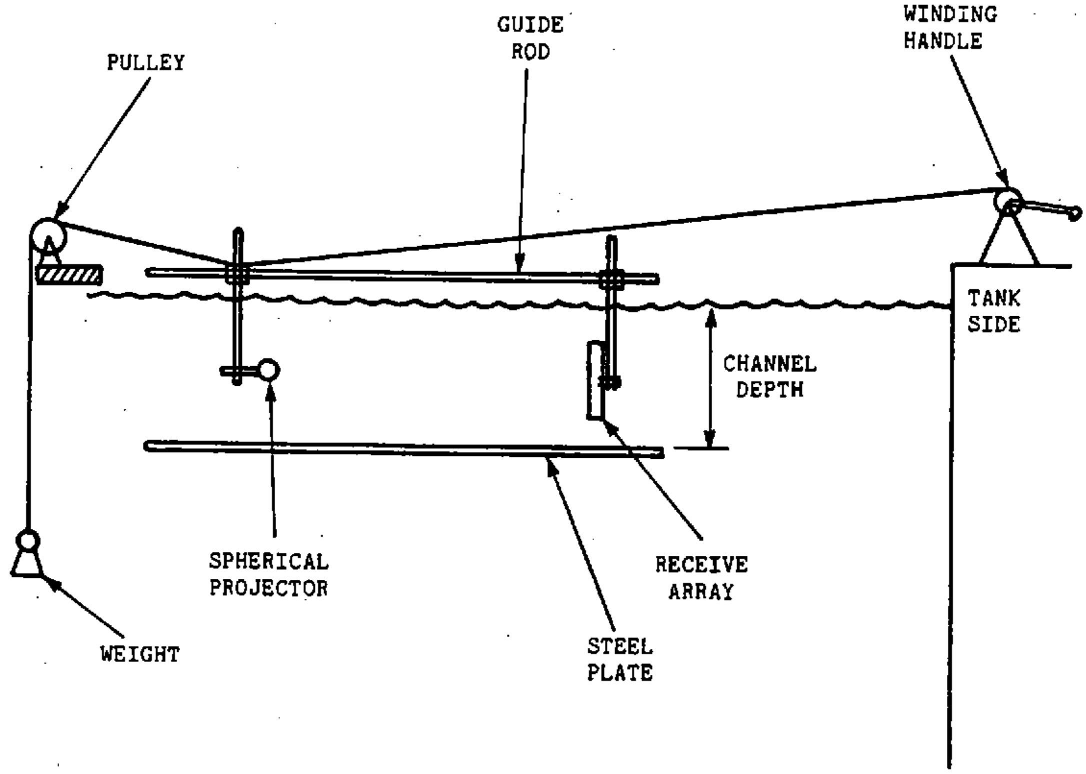

Fig. 1 Experimental Layout of the Bounded Channel

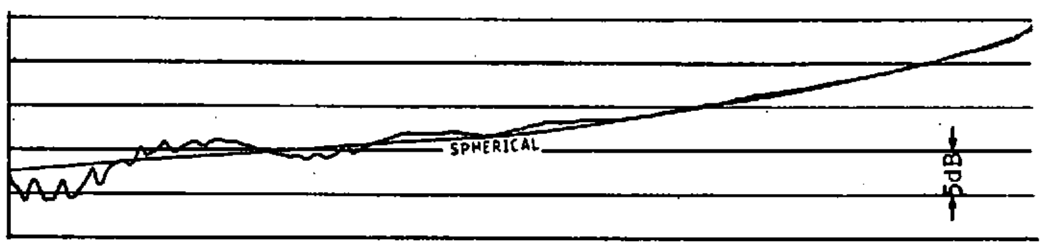

Fig. 10 Computed Binomial Array Response at 50 kHz

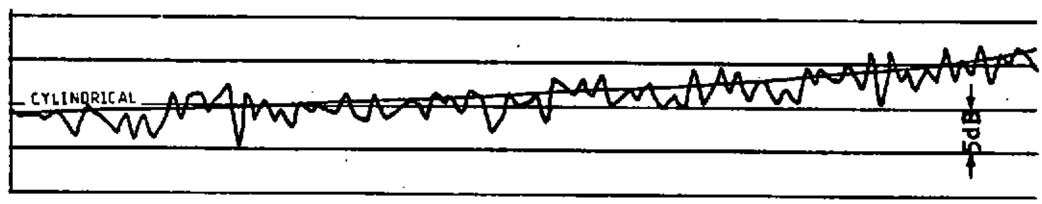

Fig. 11 Computed Array Intensity Response at 50 kHz

Fig. 2 Measured Array Response @ 50 kHz

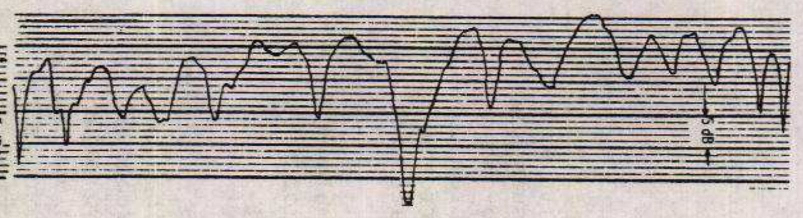

Fig. 3 Measured Point Response @ 50 kHz

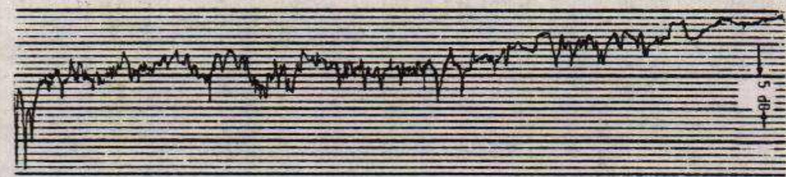

Fig. 4 Measured Array Response @ 100 kHz

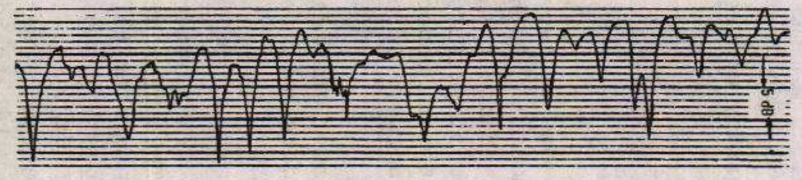

Fig. 5 Measured Point Response @ 100 kHz

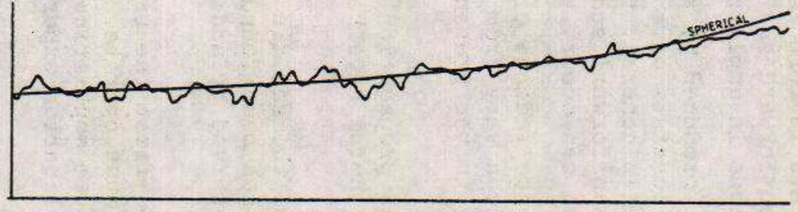

Fig. 6 Computed Array Response @ 50 kHz

Fig. 7 Computed Point Response @ 50 kHz

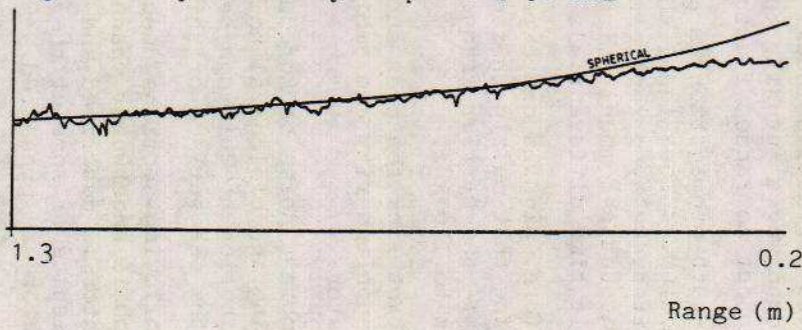

Fig. 8 Computed Array Response @ 100 kHz

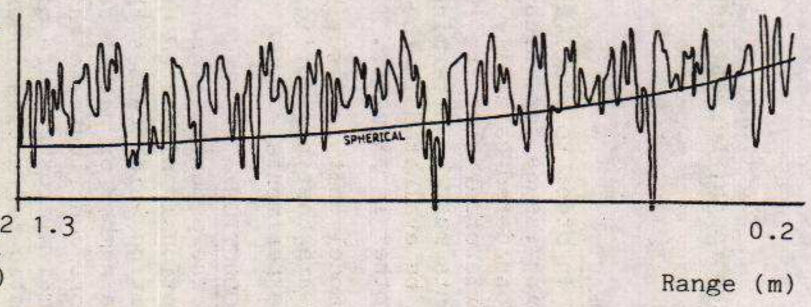

Fig. 9 Computed Point Response @ 100 kHz